Aerogels

B. M. Smirnov

Institute of Thermophysics, Siberian Branch of the Academy of Sciences of the USSR, Novosibirsk

Usp. Fiz. Nauk **152**, 133–157 (May 1987)

Contents

1. Introduction 420
2. Production of aerogels 420
3. Properties of aerogels 422
4. Sol-gel conversion 426
5. Applications of aerogels 427
6. Aerogels and ball lightning 428
7. Conclusion 431
References 432

1. INTRODUCTION

The aerogel is a peculiar physical object consisting of a macroscopic cluster of rigidly connected macroparticles. This rigid skeleton occupies only a small fraction of the cluster's volume—the rest is taken up by pores. Hence the prefix "aero" to characterize the low specific gravity of the object. The very first aerogel samples of silica, obtained by Kistler[1–4] over fifty years ago, exhibited specific gravity as low as 20 g/liter.

Although the aerogel has been a familiar object for some time, it has attracted more interest in the last decades because of its many possible applications. Let us briefly consider some of these.[5] Since it is a stable porous substance with large interior surface area, an aerogel of appropriate composition may serve as a catalyst for certain chemical processes that produce organic compounds. Also, the large interior capacity of an aerogel may be used to store certain materials, particularly rocket fuel and oxidizer.[5–7] This permits the replacement of liquid fuel with solid fuel.

The main share of currently produced aerogels (that is, silica aerogel) is used as material for Cherenkov detectors. For example, the detector at the DESY accelerator (Hamburg) has an area of 11.8 m^2 and contains 1700 liters of silica aerogel.[8–10] A number of applications of silica aerogel are due to its low thermal conductivity, which is comparable to that of gases, and also to its high transparence. These properties suggest the use of aerogel as a thermal insulator: feasibility studies of using silica aerogel for thermal insulation of windows and walls have been carried out—the limiting factor is the production cost. This is not as much of a consideration in specialized applications involving the use of silica aerogel as an insulator.

Because of its structure the aerogel has a low Young's modulus; sound velocities in aerogels are also very low, even lower than in gases. This is of interest in various acoustic applications: sound impedance lines, soundimpermeable and sound-reflecting baffles, and so forth.

Although real interest in aerogels is determined by the feasibility of practical applications, the specific physical properties of these materials deserve attention. The very process of producing aerogels from the liquid phase is interesting. The precipitating solid phase does not form a single solid mass, but a rather open structure. This situation is apparently quite common and corresponds to the formation of most porous bodies. But even in the case when the solid phase ends up as a single mass aerogel formation may play the role of an intermediate phase. For this reason aerogel formation may be of interest in the physics of solids and solutions, and in biophysics, where analogous processes take place.[11]

Aerogels are light substances. And yet the lightest practical aerogels are an order of magnitude heavier than air. However, there appear no fundamental obstacles to producing ever lighter aerogels, possibly at some cost to their strength. If an aerogel that has specific gravity comparable to air is synthesized, it may serve as a skeleton for the active material in ball lightning. Since aerogel structure is identical to that of the active material in ball lightning, such a possibility deserves attention and will be analyzed in this article.

Although real aerogels have been known for over half a century, the studies of aerogels have been limited by their relative unavailability. Yet as an interesting physical object with specific physical properties the aerogel deserves more attention. One of the aims of this article is to draw attention to this surprising object.

2. PRODUCTION OF AEROGELS

The aerogel is an object of fragile structure that is usually grown from the liquid phase; the liquid inside is subsequently drained. Therefore an aerogel may be obtained via a sequence of technological operations by maintaining appropriate process parameters. Physically, the formation of an aerogel proceeds in the following manner. In the first phase of the process one of the components in a solution precipitates into the solid phase. The precipitation occurs in a peculiar fashion: the precipitating component aggregates at many condensation centres, forming small macroscopic particles whose diameter usually exceeds the size of component molecules by an order of magnitude or more.

 0038-5670/87/050420-13$01.80

Such a process is possible if the particle growing in the solution gradually builds up a charge that prevents other molecules of the same charge from further accretion. Hence this process is possible in a small acidity interval of a given solution. Furthermore, the molecules comprising the particle must be strongly bound to each other, whereas in solution they exist as individual molecules or ions. It is therefore convenient that the molecules appear in solution as a result of slow chemical processes and that the macroscopic particle grow by the chemical, rather than physical, addition of individual molecules. This would guarantee the stability of the solid particle. Evidently the chemical character of aerogel formation plays a principal role.

The subsequent process is the aggregation of separate particles in the solution, the so-called sol-gel conversion. This process is slower than particle formation because it is determined by macroparticle diffusion. It may turn out that the charge buildup that limited macroparticle growth impedes their aggregation. Then the solution parameters have to be modified. It is quite important that the resulting cluster have a strong skeleton, for then the final aerogel product shall be mechanically stable. For this reason aerogels are prepared from a limited number of chemical compounds: the oxides of a number of chemical elements and mixtures of such oxides. To date aerogels have been prepared from Li_2O_3, B_2O_3, MgO, B_2O_3, Al_2O_3, SiO_2, TiO_2, Fe_3O_4, CuO_2, ZrO_2, MoO_2 (see Refs. 5–7, 12–16).

The last process in aerogel formation—the drying or removal of liquid molecules from the pores—is of fundamental importance. Since the aerogel has many microscopic pores liquid molecules inside these pores exert high pressures. For example, it is estimated in Ref. 17 that 2 nm diameter water molecules inside silica aerogel pores exert pressures of the order of 20 kbar. Consequently the drying of aerogels in air or vacuum creates great internal stresses which may compress or, possibly, destroy the skeleton. An aerogel produced in these conditions is known as a xerogel: it is also porous, but exhibits much higher specific gravity and much lower internal pore volume than a true aerogel.

The problem of drying aerogels was solved by Kistler[1–4] in the early 1930s. He was able to obtain silica aerogel samples and study their properties. The history of aerogels thus begins with Kistler's investigations. Kistler would dry the aerogel in an autoclave at supercritical temperature and pressure for the liquid inside the pores. The evaporation of the liquid at supercritical parameters and its replacement by gas then preserves the internal structure of the aerogel. This method became standard in the drying of aerogels.

For an example of real aerogel formation let us cite the approaches used in the preparation of the silica aerogel. The initial material in Kistler's classical method was Na_2SiO_3 salt dissolved in a hydrochloric acid solution, leading to the chemical reaction

$$Na_2SiO_3 + 2HCl \rightarrow SiO_2 \cdot nH_2O + 2NaCl. \qquad (2.1)$$

The salt precipitated out and was removed. The remaining solution was washed and filtered; then the water in solution was replaced by either ethanol or methanol, which have lower critical temperatures and pressures. Subsequently the aerogel was dried in an autoclave in supercritical conditions.

A more technological method of preparing the silica aerogel is based on the hydrolysis of tetramethoxysilane[5,6,12,18] which proceeds as follows:

$$\begin{aligned} Si(OCH_3)_4 + 4H_2O &\rightarrow Si(OH)_4 + 4CH_3OH, \\ Si(OH)_4 &\rightarrow SiO_2 \cdot 2H_2O. \end{aligned} \qquad (2.2)$$

No harmful additives are produced in this process and the solution need not be washed or filtered. In this sequence the main process of aerogel preparation may be completed in several hours. The initial material in reaction (2.2) may be replaced by other silicon compounds, such as the cheaper tetraethoxysilane, in which case the reaction would proceed as follows:

$$\begin{aligned} Si(OC_2H_5)_4 + 4H_2O &\rightarrow Si(OH)_4 + 4C_2H_5OH, \\ Si(OH)_4 &\rightarrow SiO_2 \cdot 2H_2O. \end{aligned} \qquad (2.3)$$

This method of preparing the silica aerogel, as well as methods employing different silicon compounds, has become quite popular[5,18–23]

Let us consider several features of the process that emphasize its chemical nature. Reactions (2.2) and (2.3) proceed in the presence of small quantities of HCl or HF added as catalysts. Further, gel formation in solution is to some

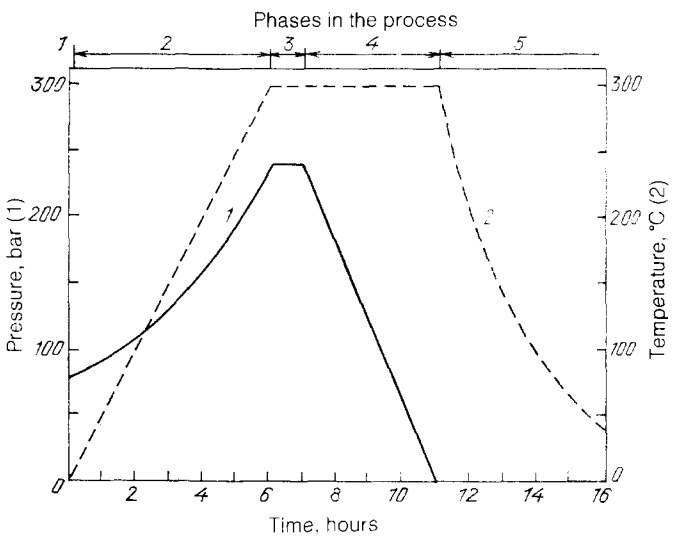

FIG. 1. Temperature and pressure as functions of time in an autoclave that produces silica aerogel from tetraethoxysilane $Si(OC_2H_5)_4$.[28] Phases in the process: 1—applying a prepressure of nitrogen (80 bar); 2—heating; 3—equilibrium; 4—vapor removal; 5—cooling.

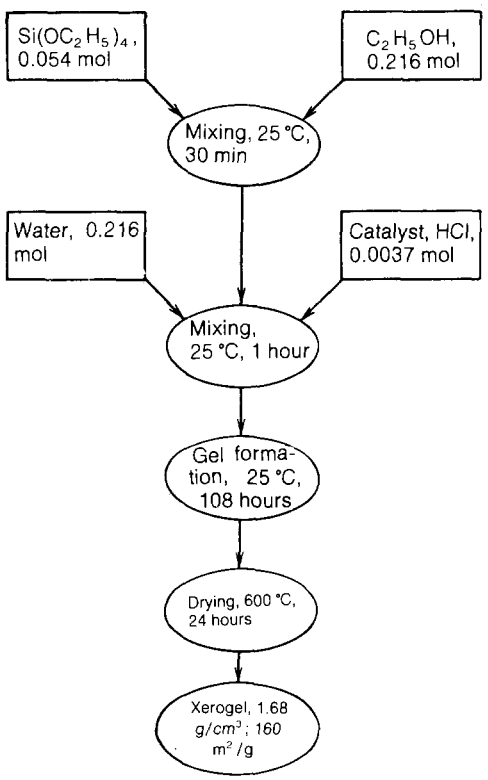

FIG. 2. Silica gel formation sequence at atmospheric pressure.[22]

extent accompanied by the hydrolysis of initial materials,[24] i.e., ions participate in the reaction. Finally, raising the temperature in the autoclave speeds up gel formation: at high temperatures gel formation takes several hours, at room temperature the process is slower. In order to illustrate the temporal nature of the process we plot in Figs. 1 and 2 the temporal characteristics of aerogel or gel formation (2.2) in an autoclave and at atmospheric pressure respectively.

Usually another production phase—annealing at atmospheric pressure—is inserted in the sequence. For example, in the production system described below[25,26] prepared silica aerogel was heated in an autoclave at the rate of 35 °C/hour up to a temperature of 500 °C, at which point it was kept for several hours. Such an operation significantly enhances the aerogel's transparence.

It should be emphasized that the production of high-quality aerogel requires significantly more time. Thus in the 98 liter autoclave[25] that produced aerogel for CERN (see below) the full cycle actually took a week and produced 50 liters of aerogel.

Another feature of aerogel production according to processes (2.2) and (2.3) that should be remarked upon is that since flammable substances are subjected to high temperatures and pressures such processes may be quite dangerous. A case in point is the instructive history of the Swedish company "Airglass" which produced silica aerogel for CERN Cherenkov detectors.[25-27] During 1979 the 98 liter autoclave which reached the temperature of 270 °C and pressure of 90 bar produced over 1000 liters of aerogel (the critical temperature and pressure of methanol are 240 °C and 78.5 bar respectively). A single cycle yielded 18 aerogel tiles of $20\times20\times3$ cm (total volume over 20 liters). Then a new, 1100 liter unit was constructed, which was supposed to produce simultaneously 100 $60\times60\times3$ cm aerogel tiles (total volume 360 liters). On August 27, 1984, after several successful cycles the unit sprung a methanol leak. An explosion followed: The autoclave building was completely destroyed and the three people inside at the time were seriously injured. Although the subsequent investigation uncovered no error on the part of the personnel, this incident could not but create psychological opposition to large-scale aerogel production technology.

3. PROPERTIES OF AEROGELS

The aerogel is made up of a system of interconnected solid particles; the volume occupied by the particles is but a small fraction of the whole. Almost the entire volume is occupied by vacant pores. The characteristic size of individual particles that comprise the aerogel is usually of the order of several nm. The simplest model of an aerogel, illustrated in Fig. 3, consists of spherical particles of approximately the same radius, with bonds at points where the spheres nearly touch. In this case the specific inside area S of the internal surface of the aerogel can be express in terms of particle radius r_0 by the formula

$$S=\frac{3}{\rho_0 r_0}, \tag{3.1}$$

where ρ_0 is the mass density of the aerogel material. In particular, for silica aerogel ($\rho_0 = 2.2$ g/cm^3) at $r_0 = 2$ nm we obtain $S = 700$ m^2/g. In most real samples of silica aerogel S is in the 300–1000 m^2/g range.

In this model, a small aerogel sample that still contains a large number of individual particles forms a fractal cluster (see Ref. 29). This structure is determined by the formation mechanism, wherein growth is accomplished by individual particles moving in the solution and sticking together. According to one of the properties of fractal clusters the mean mass density $\bar{\rho}$ of the substance inside a sphere of radius r is

$$\bar{\rho}(r)=\rho_0\left(\frac{r_0}{r}\right)^{3-D}, \tag{3.2}$$

where ρ_0 is density of cluster material, r_0 is the mean particle radius, and D is the fractal dimensionality of the cluster. This dependence implies that as we take larger aerogel volumes the pores also become larger and the relative volume occupied by solid material decreases.

Clearly in a real sample the fractal structure will manifest itself on a scale limited by $r \ll \bar{R}$. The limiting length may

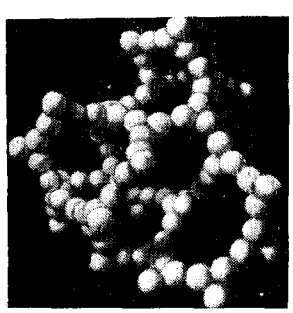

FIG. 3. The simplest model of an aerogel: spherical particles of equal radius. This structural geometry is valid at small length scales.[10]

be recovered from formula (3.2):

$$\overline{R} \sim r_0 \left(\frac{\rho_0}{\bar{\rho}}\right)^{1/(3-D)}, \tag{3.3}$$

where $\bar{\rho}$ is the mean density of material in the aerogel. Scaling law (3.3) is determined by the process of particles combining to form a gel. Early on the particles link up into small clusters, which combine and grow. As long as the clusters are small their aggregation is determined by motion in solution—resulting in a fractal structure. Later, when cluster size reaches $\overline{R}$, the clusters occupy all space and further aggregation is determined by their proximity rather than motion. Consequently at length scales $r \gg \overline{R}$ the fractal structure disappears and the cluster becomes uniform on the average.

The fractal dimensionality D of the cluster also characterizes the size distribution function of pores. Indeed, let the aerogel occupy some volume V_0 and hence have the mass ρV_0. Consider the volume contained within a distance $r \ll \overline{R}$ from the cluster. The mean density of aerogel material inside this volume is given by formula (3.2) and, since the entire mass of the aerogel is located inside, this volume has the value

$$V(r) \sim \frac{\rho V_0}{\bar{\rho}(r)} \sim V_0 \left(\frac{r}{\overline{R}}\right)^{3-D}$$

Obviously all pores smaller than or equal to r will be included in this volume. The pore size distribution function is therefore

$$df \sim r^{2-D}\, dr. \tag{3.4}$$

The most reliable method of determining the fractal dimensionality of the cluster involves small-angle x-ray or fast-electron scattering. In this case the intensity of scattering through an angle $\theta \sim 1/qr$ where q is the photon or electron wavevector yields information on the presence in the medium of elements—pores, in this case—of size r. Measurements cited in Refs. 32, 33 establish the fractal dimensionality of silica aerogel as $D = 2.12 \pm 0.05$. An analysis of data in Ref. 34 yields a somewhat larger fractal dimension (approximately 2.3).

Additional information on pore size in the aerogel may be obtained from the adsorption of various substances by the aerogel (see Refs. 6, 34–36). This information may be derived both from the dependence of the quantity of the adsorbed substance on its pressure and from the capacity of the aerogel to absorb various substances. Thus, according to data of Ref. 34, in the silica aerogel with mean density in the 0.1–0.3 g/cm^3 range, the specific volume of 1–2 nm radius pores is approximately 0.2 cm^3/g, volume of pores up to 10 nm is in the 0.6–0.8 cm^3/g range, and volume of pores up to 30 nm is in the 1.2–1.8 cm^3/g range. In these samples the total specific volume of pores, mostly determined by pores of larger radius, is 3–9 cm^3/g—inversely proportional to the aerogel's mean density. When the aerogel adsorbs water vapor in humid air the larger pores are the ones occupied.

The adsorption of various sorbents determines the size of the pores since different components are adsorbed by pores of different size. Thus, according to Ref. 6, in appropriate circumstances nitrogen is adsorbed by pores whose radius is smaller than 20 nm, whereas mercury is adsorbed by pores whose radius is larger than 6 nm. This yields information on the specific volume of pores of a given size in the adsorbent under study. For example, in Table I we present the sorbing characteristics of a number of amorphous Al_2O_3 aerogel samples.[6] Evidently an increase in the mass density of the sample decreases the specific volume of larger pores that are responsible for mercury adsorption. The specific volume of smaller pores, responsible for nitrogen adsorption, remains practically constant.

We can introduce the mean radius of pores responsible for the adsorption of a given component in a manner similar to the derivation of formula (3.1). Following standard practice, take the pores to be cylindrical. Then the mean pore radius r can be obtained from the relation

$$\bar{r} = \frac{2V}{S}, \tag{3.5}$$

where S is the specific internal surface area; V is the specific volume of the adsorbed component. In Table I we cite the mean radius of nitrogen adsorbing pores in aerogel samples. The result is consistent with earlier observations: these pores are small and their size is independent of the aerogel density.

A quantitative idea of the aerogel microstructure can be extracted from the cited data. To this end in Table II we present the sample parameters measured and analyzed in Ref. 38 (cylindrical samples of diameter up to 8 cm). The first three columns of data in Table II are taken directly from Ref. 38: specific surface area was obtained from nitrogen adsorption; particle radius was found by TEM (transmission electron microscopy).

This last method exaggerates particle size because large particles contribute more to the intensity of the scattered signal. The photographing of silica aerogel samples by TEM or scanning electron microscopy (SEM)[23] favors particles of large radius. For SEM photography the aerogel was tinted with OsO_4. The mean radius of particles turned out to be 20–30 nm. Tewari and co-workers[23] note, however, that SEM photography favors larger particles and that the obtained value may be taken as the upper bound for the particles radius.[1)] Transmission photography signals the presence of both

TABLE I. Parameters of adsorption of nitrogen and mercury by Al_2O_3 aerogel.[6]

Mass density, g/cm^3	Specific internal surface area, m^2/g (from nitrogen adsorption)	Specific volume		Mean pore radius, nm [formula (3.5)]
		Nitrogen adsorption	Mercury adsorption	
1. 0.015	470	1,25	17,3	5,3
2. 0,02	616	1,30	13,7	4,2
3. 0,04	506	1,17	10,7	4,6
4. 0,06	530	1,18	9	4,4

TABLE II. Microstructure parameters of silica aerogel samples.

Mass density, g/cm³	Specific internal surface area, m²/g	Particle radius, nm		Maximum pore size, nm [formula (3.3) and (3.1)].
		TEM photography	Formula (3.1)	
1. 0,03	1590	4	0,9	120
2. 0,05	1080	5	1,3	100
3. 0,15	520	10	2,6	55
4. 0,16	740	4	1,8	35

small particles with radius smaller than 2 nm and large particles with radius greater than 10 nm. At the same time, it follows from the value of the specific internal surface area of the sample (890–960 m^2/g) that the mean particle radius should be 1.4–1.5 nm.

Let us note another feature of aerogel structure. The density of actual samples of silica aerogels and xerogels may differ by two orders of magnitude and yet the specific internal surface area usually spans a narrow range of values. The specific internal surface area of silica xerogels is about equal to that of the corresponding aerogel and varies only weakly with density (see, for instance, Ref. 39). Hence it follows that all these structures are made up of particles of approximately the same size. The variation in specific gravity of a sample is due to the presence of large pores, whereas the specific internal surface area is due to small pores whose concentration does not change.

The pore size distribution may be used to determine the fractal dimensionality of the aerogel in the $r_0 \ll r \ll \bar{R}$ range. Pores of this size occupy a small fraction of the total pore volume and are described by the size distribution formula (3.4). Applying this formula to data on five silica aerogel samples in Ref. 35 yields $D = 2.3 \pm 0.1$, in rough agreement with the more accurate result cited above that is valid for silica gel in solution.

Let us compare the fractal dimensionality of an aerogel with that of a cluster at the stage of cluster aggregation when smaller clusters sequentially link up to form a large cluster.[56,57] In the latter case, computer modelling of the process yields 1.77 ± 0.03 for the fractal dimensionality of the large cluster.[29] This result was experimentally corroborated by Weitz and Oliveria,[86] who studied the aggregation of 7 nm gold particles in solution. The resulting clusters exhibited fractal dimensionality $D = 1.77 \pm 0.10$.

This apparent contradiction between the fractal dimensionalities of the aerogel and the cluster formed during cluster-cluster aggregation was explained by a subsequent series of experimental investigations[87–90] on cluster formation by 8–11 nm gold and silica particles in appropriate solutions. These experiments suggested a more complicated physical picture of cluster formation. More precisely, if the conditions in the solution are conducive to rapid cluster formation (on a time scale < 1 min) the resulting cluster is characterized by fractal dimensionality of 1.75 ± 0.05—this regime is known as DLCA (diffusion limited cluster aggregation) and was described earlier in section 3 of this article. The other regime, in which cluster formation is hindered and proceeds relatively slowly (on a time scale > 24 hours), produces clusters characterized by fractal dimensionality of 2.2 ± 0.05 This regime is known as RLCA (reaction limited cluster aggregation); it is the more stable of the two. Dimon and co-workers[90] have shown that clusters with $D = 1.75$ that are formed in a fresh solution evolve over several days into clusters with $D = 2.2$. Evidently the character and time scale of aerogel formation correspond to the slower regime, which in turn produces a more stable skeleton that has fractal dimensionality of 2.1–2.2 in solution. Possibly the fractal dimensionality of the skeleton increases slightly during the drying of the aerogel.

The strength and thermal stability of aerogels is also of interest. Already in his earliest studies Kistler noted that silica aerogel samples do not change up to temperatures of 700 °C, whereas at 900 °C their porosity decreases. A good understanding of the aerogel's densification may be gained from the data of Ref. 38, presented in Table III. When heated up to 800 °C silica aerogel does not change. At higher temperatures particles become larger and porosity decreases, with the attendant increase in the aerogel's density.

Young's modulus of an aerogel decreases during densification, since the latter process depletes the number of "chains" that counteract external pressure. The dependence of Young's modulus E on the aerogel density may be taken as follows

$$E = E_0 \left(\frac{\rho}{\rho_0}\right)^{\beta}. \tag{3.6}$$

Experimental data of Ref. 42, which encompass silica aerogel, xerogel, and glass, yield $\beta = 3.7$, in agreement with the

TABLE III. Silica aerogel densification when heated to 1250 °C. duration of heating—12 min.[38]

Temperature, °C	Gel density, g/cm³	Specific internal surface area, m²/g	Particle radius, nm (TEM photography)
1. 300	0,16	740	4
2. 800	0,16	780	4
3. 1150	0,27	530	5
4. 1200	0,66	160	6
5. 1210	1,00	76	12
6. 1225	1,41	36	20

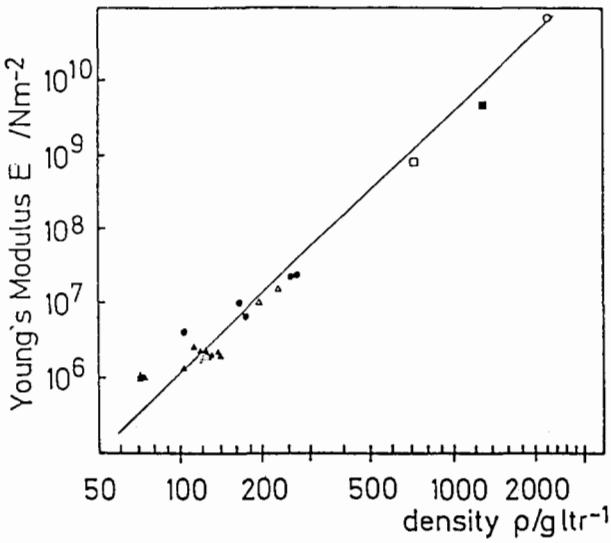

FIG. 4. Young's modulus E for aerogel and silica glass as a function of density ρ. The line represents the scaling law (3.6) for percolating systems. The symbols are: ▲—DESY tiles, ●—Lund tiles, △—BASF granules, ○—silica glass, □ and ■ are silica gels.

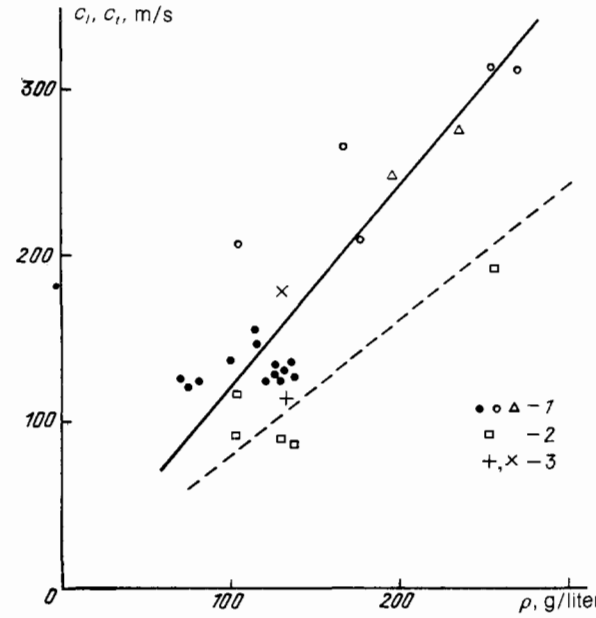

FIG. 5. Sound velocities c_l,c_t in silica aerogel. 1—measured longitudinal sound velocities in various samples;[42] 2— measured transverse sound velocities;[42] solid and dashed lines—scaling law (3.8) for longitudinal and transverse sound waves obtained from data in Ref. 42; 3—longitudinal and transverse sound velocities calculated from formula (3.7) using data from Fig. 4.

theory of Ref. 41. In Fig. 4 we plot Young's modulus against density for the aerogel only.[42] An analysis of these data yields the following values of the parameters in (3.6): $E_0 = 10^{6.58\pm0.18}$ N/m^2, $\beta = 2.8 \pm 0.2$ for $\rho_0 = 0.13$ g/cm^3. This last value for parameter β in (3.6) is probably more accurate.

The values of Young's modulus may be used to determine the speed of sound in the material. The longitudinal c_l and transverse c_t sound velocities are defined by the relations[46]

$$c_l = \left[\frac{E(1-\sigma)}{\rho(1+\sigma)(1-2\sigma)}\right]^{1/2}, \quad c_t = \left[\frac{E}{2\rho(1+\sigma)}\right]^{1/2}, \qquad (3.7)$$

where σ is the Poisson coefficient. In Fig. 5 we plot the sound velocities in an aerogel.[42] If, by analogy with scaling law (3.6), we suppose the speed of sound to obey the expression

$$c = c_0 \left(\frac{\rho}{\rho_0}\right)^{\alpha}, \qquad (3.8)$$

then an analysis of experimental data yields the same coefficient α for the longitudinal and transverse sound waves: $\alpha = 0.9 \pm 0.2$. Further, for $\rho_0 = 0.13$ g/cm^3 we obtain $c_0 = 170 \pm 30$ m/s for the longitudinal sound wave and $c_0 = 110 \pm 20$ m/s for the transverse. In silica aerogel the Poisson coefficient is

$$\sigma = 0.12^{+0.24}_{-0.12}.$$

Observe that formulae (3.7) lead to the following connection between the exponents in (3.6) and (3.8): $\beta = 2\alpha + 1$. Obviously, the value $\beta = 3.7$ does not agree with measured sound velocities, whereas $\beta = 2.8$ not only satisfies the density scaling of sound velocities but ensures quantitative agreement between velocities calculated from (3.7) and those measured experimentally (Fig. 5). Remarkably, sound velocities in real aerogel samples of low density are markedly lower than in solids and lower even than in gases. This is of interest for the corresponding practical applications.

Formula (3.6) allows us to estimate the range of densities for which an aerogel can exist in the atmosphere. Suppose that the aerogel is destroyed if its relative change in length is of order unity and the pressure gradients correspond to a human shout (80 decibels), i.e., the sound pressure amplitude is 0.2 N/m^2. When plugged into formula (3.6) these parameters yield the limiting aerogel density $\rho \sim 0.4$ g/liter. Together with other estimates, this demonstrates that in principle one may prepare an aerogel with specific gravity comparable to air.

The thermal conductivity of an aerogel is also relatively small. Thermal conductivity coefficient of silica aerogels in the 0–100 °C temperature range is 10–20 mW/m$^2 \cdot$K[43] (for comparison, the thermal conductivity of air at room temperature is 26 mW/m$^2 \cdot$K). In aerogels radiative heat transfer contributes noticeably to the total: according to Ref. 44 the coefficient of radiative thermal conductivity varies from 2 to 8 mW/m$^2 \cdot$K in the 10–90 °C temperature range. Silica aerogel absorbs strongly near the 7.5 μm wavelength, whereas in the 4–7 μm wavelength range it is practically transparent. Absorption near 7.5 μm results in a strongly temperature dependent ($\sim T^{5/6}$) radiative thermal conductivity coefficient.[44]

Silica aerogels are based on a transparent material. Thus it may be expected that real samples, with their low densities, will be even more transparent. But the disordered particle distribution in the aerogel coupled with the effect of impurities[2)] lead to significant light scattering. For example, the specific optical density of silica aerogel at the 0.55 μm wavelength is 11 ± 3 cm^2/g.[35] This implies that half the incident light in sample 1 of Table II would be lost after passing through 2 cm of material.

Since the transparence of an aerogel is determined by the material structure, it may depend on the parameters of

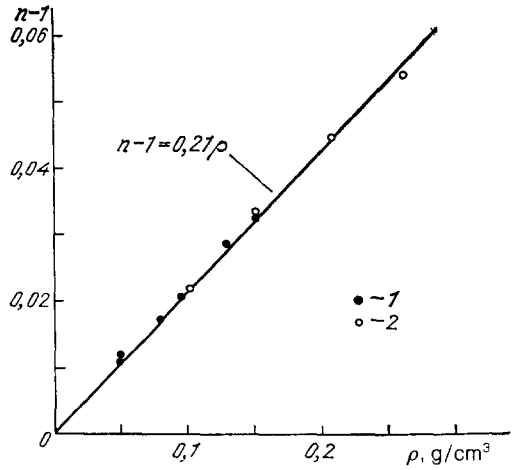

FIG. 6. Refractive index of silica aerogel.[10] Measurements: 1—Ref. 9; 2—Ref.25. Straight line: $n - 1 = 0.210\,\rho$.

the production process. Refs. 10, 19 state that increasing the gel formation time significantly enhances the transparence of the sample.

The specific gravity of an aerogel places it somewhere between a solid and a gas. This also holds for the refractive index n (Fig. 6), which is close to unity but still larger than the index in gases. According to Refs. 9, 10, 25:

$$n - 1 = (0.210 \pm 0.002)\,\bar{\rho}, \tag{3.7}$$

where $\bar{\rho}$ is the aerogel density in g/cm^3. Note that in pure silica glass the quantity $(n-1)/\rho$ is 0.207 cm^3/g.

4. SOL-GEL CONVERSION

The key process in the preparation of an aerogel is the formation of the gel—the cluster of linked macroparticles. This process also plays an important role in the production of glasses,[50–53] since the resulting structure exerts an influence on the properties of the finished product. The same process is important in biophysics,[11,54] where it is responsible for a class of structures. Generally, gel formation in solution is inseparable from the accompanying electrochemical processes which fix the chemical composition and structure of the new phase, and determine the time required. Nonetheless we shall neglect these processes in our discussion of gel formation. This will permit us to estimate the maximum speeds of gel formation, and also gain insight into the nature of the process in real systems and the possibilities of controlling it.

Accordingly we suppose that the medium in which gel formation takes place is neutral, i.e., has no effect on the properties of the particles it envelops. During the first, condensation phase a large number of macroparticles—sols—forms in the medium, each containing many molecules. We are interested in the next phase—the sol-gel conversion, i.e., the aggregation of macroparticles into a cluster. This process is driven by the motion of macroparticles and is consequently slower than the preceeding macroparticle formation which is driven by the motion of individual molecules. Therefore we may assume that the sol-gel conversion, i.e., the aggregation of macroparticles into a cluster, occurs when all individual molecules of the gel component are incorporated into macroparticles.

We note that this model can be employed in analyzing the formation of other porous materials, such as silica gel zeolites and activated carbons. The separation of phases or components in those systems occurs via the formation of clusters of individual particles. The subsequent removal of the weakly linked component leaves the other component in the form of a hard skeleton with pores.

The growth of a cluster composed of individual particles may follow two distinct sequences. One involves a single cluster growing when individual particles stick to it.[55] In the other, many clusters form first and then link up, so that the characteristic cluster size increases while the number of clusters falls with time.[56,57] We shall consider both alternatives, although the latter is more applicable to our case.

Suppose for simplicity that all particles are spheres of the same size and that any two particles or clusters stick together upon touching. We take into account the diffusive motion of particles in the medium and also the diffusive motion of clusters, as well as their downward motion due to gravity. For simplicity we also suppose that the medium's resistance to a cluster is the same as to a spherical particle of the cluster's dimensions. Let us derive the quantitative characteristics of gel formation within this framework of assumptions.

First consider the process wherein a single cluster grows as individual particles stick to it. The number of particles in the cluster η satisfies the equation

$$\frac{dn}{dt} = \nu_0 + \nu_1, \tag{4.1}$$

where ν_0 is the rate at which the cluster acquires particles due to their Brownian motion and ν_1 is the rate at which the cluster captures particles as it falls due to gravity. For simplicity take the particles comprising the cluster to be identical. The radius of the cluster R and the number of particles in it n are connected by formula (3.2) and hence

$$n = \left(\frac{R}{r_0}\right)^D, \tag{4.2}$$

where r_0 is the radius of a single particle and D is the fractal dimensionality of the cluster.

The rate of particles sticking to the cluster because of their diffusive motion is given by Smoluchowski's formula[58] (see also Refs. 29, 59):

$$\nu_0 = 4\pi \mathscr{D} R N, \tag{4.3}$$

where $\mathscr{D}$ is the diffusion coefficient of particles in the medium; N is their number per unit volume. If the size of the particles exceeds their mean free path in the medium, the diffusion coefficient equals

$$\mathscr{D} = \frac{T}{6\pi r_0 \eta}, \tag{4.4}$$

where T is the temperature of the medium in energy units and η is the medium viscosity. From (4.4) and (4.3) we then have

$$\nu_0 = k_0 N n^{1/D}, \tag{4.5}$$

where the rate constant $k_0 = 2T/3\eta$ is independent of the nature and size of the particles. In air at $T = 300$ K this constant is $1.5 \cdot 10^{-10}$ cm^3/s; in water at that temperature it is $3.2 \cdot 10^{-12}$ cm^3/s.

The capture rate of a falling cluster is

$$\nu_1 = \pi R^2 v N, \tag{4.6}$$

where v is the velocity of the cluster's gravitational fall. Modelling the cluster as a spherical particle we have[60]

$$v = \frac{2\rho g}{9\eta},$$

where ρ is the difference in density between the particle material and the medium. In this derivation we implicitly use the fact that the pores in the cluster are filled by the medium in which it grows. For the capture rate ν_1 we then obtain

$$\nu_1 = k_1 N n^{(D+)1/D}, \tag{4.7}$$

where

$$k_1 = \frac{2\pi\rho g r_0^4}{9\eta}.$$

Substituting (4.5) and (4.7) into equation (4.1) we find the growth time of the cluster

$$t = \frac{1}{N}\int \frac{dn}{k_0 n^{1/D} + k_1 n^{1+1/D)}}. \tag{4.8}$$

Taking $k_0 \gg k_1$ we find that this integral is convergent if $n \sim k_1/k_0$ so the limits of integration in (4.8) may be taken as 0 and ∞. Computing the integral with the assumption that the number of particles in the growing cluster $n \gg k_1/k_0$, we obtain the growth time

$$t = \frac{\pi}{N k_0^{1/D} k_1^{(D-1)/D} \sin(\pi/D)}. \tag{4.9}$$

A more realistic physical picture of the sol-gel conversion involves the aggregation of particles into small clusters and the subsequent linking of these small clusters.[56,57] As in the preceeding scenario the clusters grow with time, but now the process is modified by the absence of individual particles. Utilizing the same aggregation mechanisms we may recast expressions (4.4) and (4.6) into appropriate aggregation rates which take the form

$$\nu_0 = 4\pi (\mathscr{D}_1 + \mathscr{D}_2)(R_1 + R_2) N_2,$$
$$\nu_1 = \pi (R_1^2 + R_2^2) \mid v_1 - v_2 \mid N_2;$$

where the indices 1 and 2 refer to the two combining clusters while the rates themselves characterize the balance for clusters of the first kind.

By using a simple cluster size distribution function we obtain, instead of (4.1), the following equation for the mean number of particles n_0 in a cluster

$$\frac{dn_0}{dt} = N_0 k_0 a_0 + N_0 k_1 a_1 n_0^{1+(1/D)}; \tag{4.10}$$

where N_0 is the initial particle density; rate constants k_0 and k_1 were defined earlier ($k_0 = 2T/3\eta$, $k_1 = 2\pi\rho g r_0^4/9\eta$); and the numerical constants a_0 and a_1 are fixed by the cluster size distribution function—for the simple distribution function they are $a_0 = \pi + 2$, $a_1 = 2.7$. We now find the gel formation time

$$t = \int_0^\infty \frac{dn_0}{N_0 (k_0 a_0 + k_1 a_1 n_0^{1+(1/D)})}$$

$$= \frac{\pi D}{(D+1)\sin[\pi/(D+1)]\, N_0 (k_0 a_0)^{1/(D+1)} (k_1 a_1)^{D/(D+1)}}. \tag{4.11}$$

The mean density of the cluster material falls as the cluster grows. When the clusters reach the characteristic size $\bar{R}$ at which the mean density of the material inside becomes approximately equal to the total mean density in the volume, the clusters come to occupy the entire volume. The subsequent linking of clusters into a single gel will be determined by their proximity; the fractal properties of the gel will only manifest themselves at distances not exceeding $\bar{R}$ and the same quantity will limit the size of the pores in the resulting gel.

Note that the gel formation times derived above apply to the scenario wherein small particles aggregate because of their diffusion in the medium while larger clusters aggregate due to their motion in the gravitational field. This occurs when the condition

$$r_0^4 \ll \frac{T}{\rho g} \ll \bar{R}^4, \tag{4.12}$$

holds where r_0 is the initial radius of the particles; ρ is the difference in mass densities between the particle material and the medium; g is acceleration due to gravity; and T is the medium temperature in energy units. If the right half of the inequality is not satisfied the second aggregation mechanism is negligible and equation (4.10) yields the following result for the gel formation time

$$t \sim \frac{n_0}{N_0 k_0 a_0} \sim \frac{1}{N_0 k_0 a_0}\left(\frac{\rho_0}{\bar{\rho}}\right)^{D/(3-D)}, \tag{4.13}$$

where ρ_0 is the mass density of the particle material and $\bar{\rho}$ is the mean mass density of the entire system.

In order to appreciate the actual time scales involved let us carry out some numerical estimates. We take the lowest possible concentration of the condensing substance such that the specific gravity of the aerogel matches the specific gravity of air. Although the specific gravity of real samples is markedly greater, our assumption leads to reliable qualitative conclusions. In silica aerogel with particle radius $r_0 = 10$ nm and cluster fractal dimensionality $D = 2.12$ we obtain from formula (4.9) the room temperature result $t = 1.2$ s if the process takes place in air and $t = 76$ s if it takes place in water. In the cluster-cluster model, formula (4.11) yields for these parameters corresponding gel formation times of 3.5 s and 4 min. The latter mechanism results in longer times because cluster aggregation reduces their density. Observe that in this example $\bar{R} \sim 5$ μm according to formula (3.2), whereas $(T/\rho g)^{1/4} = 0.7$ μm, and hence condition (4.12) is satisfied.

Evidently the times required for cluster formation within the framework of the treated models underestimate true gel formation times by two to three orders of magnitude. This indicates that the aggregating particles are charged, which markedly impedes the process. Similarly, we can conclude that it is possible to speed up gel formation considerably by changing the state of the solution after the particles have formed.

5. APPLICATIONS OF AEROGELS

The production and investigation of aerogels took place in the course of studies devoted to glasses. But aerogels are expensive, costing about 9 dollars per gram,[61] and for this reason aerogel applications are limited. In particular, they

cannot be used as raw materials for glasses with specific properties, although in principle this possibility exists.[51] In fact only a part of the sequence developed for the technological production of aerogels is used for that purpose: the main physical process—sol-gel conversion—is of practical interest because it permits the production of stable configurations of oxides of a number of metals and elements, as well as their mixtures in controlled proportions.[49-53] In particular this method is used for producing films and coatings for glasses, mirrors, and reflectors in special applications.

Currently the main application of aerogel is in Cherenkov detectors for the analysis of fast hadrons: protons, π-mesons, K-mesons.[10,25-28,37,40,47,48,53,68,85] A large class of Cherenkov detectors of various sizes uses aerogels, and good results obtained by such detectors tend to increase their numbers. The plans for space missions now include aerogel Cherenkov detectors.[62-64] These aerogel applications are perfectly sensible: in high-energy research and astrophysics the question of cost is less important than in other areas. Today the detector applications of aerogel are largely due to one of its less interesting features—the near-unity index of refraction. Yet most of the currently produced aerogel is used for such purposes, whereas other applications which could employ unique aerogel properties are still in the research and development stage.

Aerogel possesses great internal capacity. In an aerogel the volume occupied by pores may exceed that occupied by material by a factor of ten or more. Consequently aerogels may be used to store various substances. In particular, silica and Al_2O_3 aerogels, as well as an aerogel based on their mixture, have been used to store components of rocket fuel: nitric acid as the oxidizer and unsymmetric dimethylhydrazine as fuel.[5-7] These materials occupy the aerogel pores and the stored weight may significantly exceed the weight of the aerogel itself. It was experimentally demonstrated that 1 g of aerogel can store 20 g of nitric acid and 40 g of unsymmetric dimethylhydrazine.

Also important is that the aerogel is a porous substance with controllable chemical composition. Thus it may be used as a catalyst.[5-7,13,65-67] Aerogel has many merits as a catalyst: various metals can be introduced into its composition and it is quite stable chemically. For these reasons aerogels have been successfully used as catalysts in reactions involving organic compounds.[5-7,13,65-67] The number of reactions in which aerogels are useful as catalysts will certainly increase with the years to come.

Aerogels are porous substances with controllable chemical compositions. Various additives are easily introduced and it is easily compressed into a solid. Consequently aerogels may be employed to produce various types of glasses (solid and porous, single- and many-component) and other composite materials with specific properties.[7]

It turns out that the aerogel's ability to absorb moisture quickly can be used to destroy insects, who lose bodily fluids to the aerogel.[5,6] Accordingly, aerogels may be used as insecticides that do not chemically affect the environment.

Since aerogels are transparent and have low thermal conductivity, they are very good thermal insulators. Many studies and evaluations have considered the use of aerogels to insulate various parts of buildings.[69-73] These applications appear impractical because of aerogel's high cost. But in special devices, especially those intended for work in space, the insulating properties of aerogels may be put to good use.

The same is true of the acoustic applications of aerogels. Since sound travels more slowly in aerogel than in air, the acoustic properties of aerogels could find many applications in acoustic impedance lines, sound reflectors, soundproof baffles and so forth. Once again, however, the high cost of aerogels restricts these applications to special devices and systems.

This brief discussion of aerogel applications is necessary to appreciate the true significance of the object. On the one hand, aerogels are unusual objects with specific physical properties which may be utilized in practical applications. On the other hand, aerogels are expensive, which restricts their use in areas adapted for aerogel applications. This, in turn, dampens the interest in aerogels as physical objects. Thus we find ourselves in a contradictory situation.

6. AEROGELS AND BALL LIGHTNING

The aerogel structure is similar to the material that makes up ball lightning. In this respect the aerogel is an analog of ball lightning, modelling its structure much like pyrotechnic compounds model its luminescence due to chemical transformations. There is a natural desire to unify these two elements to obtain a model of ball lightning. Since the aerogel forms a light and strong skeleton a model of ball lightning might propose that the active material in ball lightning is adsorbed by an aerogel. This, in fact, is a variant of the model in which the active material of ball lightning is adsorbed by a porous substance.[74] Before proceeding to analyze the tenability of this theory let us consider some features of ball lightning[29,75] that stem from an analysis of observational data and comparison with the appropriate class of physical processes.

First of all, the material in ball lightning is organized in a filamentary structure;[76,77] a closer examination reveals it to be a fractal cluster like the aerogel.[29] Further, in ball lightning energy is realeased via chemical reactions, i.e., energy storage in ball lightning is chemical in origin.[78] Finally, the luminescence of ball lightning is analogous to that of flare compounds used in pyrotechnics. Chemical reactions drive the temperature of certain points in the skeleton to high values $T > 2000$ K, resulting in skeleton luminescence due to resonantly excited atoms of additives in the mixture. At the same time, since the probability of quenching of excited atoms is near unity in atmospheric air the luminescent regions are in equilibrium. This implies that the relative number of excited atoms is determined by the local air temperature in the region and is independent of the method of excitation.

Without dwelling on other aspects of ball lightning let us analyze the model at hand: the strong skeleton of ball lightning is made up of an aerogel in which the active material is adsorbed. Let us also note the following consideration: oxides are the most likely candidates for the material that makes up the ball lightning's skeleton. They form strong chemical bonds and can link up in the structure of ball lightning. All this information derives from the study of aerogels. Also, the first fractal clusters to be studied[80] were obtained by evaporating iron, zinc, and silica in air, with the fumes relaxing to form oxides. These considerations imply that the

skeleton of ball lightning is made up of oxides. Hence the structure is similar to an aerogel, only more porous. This last fact is not of fundamental significance because the strength of practical aerogels must satisfy more stringent requirements than the active material in ball lightning.

First, let us consider the electrical properties of ball lightning modelled by an aerogel. The interaction of ball lightning with metallic objects and electric devices, as well as the electric effect it has on human beings, indicate that ball lightning carries electric charge.[82] This charge creates surface tension in the ball lightning material, ensuring its stability and spherical shape.[77] In subsequent evaluations we will take the surface tension of ball lightning to equal that of water at room temperature (0.07 J/m^2). Since the average ball lightning radius is 14 cm, this corresponds to total charge of $5\cdot10^{-7}$ C, surface electric field of 2.4 kV/cm, and electric potential of 34 kV. If we divide the total charge by the ball lightning volume we obtain the volume charge density of $3\cdot10^{8}$ cm^{-3}. The electric energy of the sphere is 0.02 J.

Let us analyze the above values from the point of view of a the formation dynamics of charged cluster. The difference in the mobilities of positive and negative ions in air bestows negative charge on individual particles in air plasma. Equilibrium charge of a particle is proportional to its radius and independent of the charged particle density in the plasma. For a particle of 3 nm radius in ordinary air this charge is $-0.04\pm0.01\,e$. (This implies that 4% of the particles have charge $-e$ while the rest are neutral.) The charge to mass-ratio for such a particle is 0.03 C/g. Worth noting is that if the aerogel density equals that of air then the above charge and parameters of ball lightning lead to a ratio of $3\cdot10^{-8}$ C/g, i.e., the quantity of charge in ball lightning presents no problem. In addition, studies have shown that the charge on the particles does not significantly affect their aggregation. Two problems arise. First, as the cluster grows its equilibrium charge decreases and hence there must be discharges in the plasma. Second, the density of charged particles in ordinary air is usually 10^2–10^3 cm^{-3}, several orders of magnitude lower than our estimate of charge density in ball lightning. This implies that before the clusters are formed there is concentration of charge and spatial separation of negatively charged particles from positively charged ions.

Estimates show that charge buildup in ball lightning cannot proceed as in clouds, where negatively charged droplets fall under their own weight. In ball lightning the particles are much smaller and the necessary field intensities are much larger, so the cloud mechanism is negligible. As a consequence, charge separation can occur only under the influence of external electric fields. The mobility of 3 nm radius particles in air is about three orders of magnitude lower than the mobility of molecular ions and hence solid charged particles cannot participate in charge separation. It is possible to estimate that in the course of building up the charged system charge separation occurs over milliseconds under the influence of fields of the order of 10 kV/cm.

The buildup of charge in ball lightning can be visualized in this manner. In our material electric effects create a plasma of charged particles with density $N\gtrsim10^{19}$ cm^{-3}. The plasma contains a large number of solid particles. Then an equilibrium negative charge of solid particles is established in the aerial plasma over a period $\tau\lesssim2\cdot10^{-4}$ s, followed by charge separation induced by external fields on a time scale of 10^{-3} s.

Let us examine a model of ball lightning in which the skeleton is made up of oxides and resembles a dilute aerogel, whereas the active material is stored in some of the pores. The evolution of such a system may be described as follows. At any given time chemical reactions proceed at some points in the system, heating up the surrounding material and causing luminescence. Waves of chemical reaction propagate through the active material: the reaction commences at some points and ceases at others, but at any given time there is a large number of luminous regions creating the impression that the whole volume is luminous.

The plausibility of a model can be ascertained by quantitatively computing its parameters. We will cite a number of computations, based on the observed parameters of ball lightning, and characterize the processes that occur in our ball lightning model. The observed parameters are obtained from an analysis of much experimental observation, which is amply presented in Barry's and Stakhanov's texts.[81,82] Such information permits us to gain a clear understanding of ball lightning as an observational phenomenon. Furthermore, in analyzing our model we employ the average parameters of ball lightning.[29,75] They are: 14 cm radius, 20 kJ energy, 9 s lifetime, 1400 lm radiant flux. These yield ball lightning energy density of 2 J/cm^3, power of 2 kW, and light output of 0.7 lm/W (Fig. 7).

Remarkably, the energy of an average ball lightning equals that of a dozen matches. If the active material of ball lightning is modelled by yellow flare compound,[79] the energy output will be satisfied by about 3 grams. If this material were uniformly distributed over the volume of an average ball lightning, the specific gravity of active material would be about 5 times less than ordinary air. The light output of

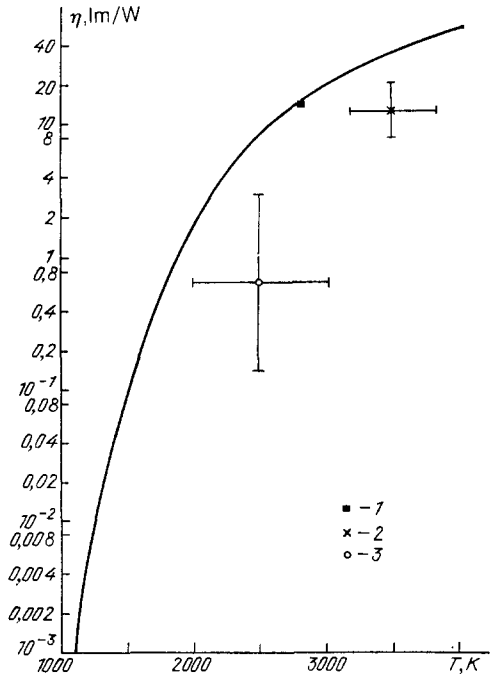

FIG. 7. Light radiated as a function of the object's temperature. Solid curve corresponds to ideal black-body radiation; 1—electric lamp; 2—pyrotechnic flare compounds; 3—ball lightning.

the yellow flare compound is 8 lm/W, exceeding ball lightning by an order of magnitude.

Air flow through the system from the bottom up sets the gas dynamics.[29,83] This flow provides the lift for ball lightning, as well as the heat sink. Experimental modelling of the gas dynamics in such a system[83] reveals that given our chosen parameters of size and power output, the air inside is heated by 60 K on the average. Consequently, although the regions of active chemical reaction are quite hot, $T > 2000$ K, the heating of the entire system is moderate on the average.

Let us follow the propagation of chemical reaction (combustion) waves and luminescence waves. Phenomenologically these processes may be understood as follows. Strongly exothermal chemical reactions are preceeded by an inductive period. After the combustion of material at a given point, the wave of combustion propagates through active material along its filaments. The reaction proceeds simultaneously at many points in the skeleton. Since the reaction products are very hot, the chemical process is accompanied by luminescence; since this occurs simultaneously at many points, it appears that the whole ball lightning is luminous. Upon reaching some point in the skeleton the reaction may cease and start up somewhere else. The luminescence then does not appear steady. Let us numerically evaluate this process, modelling the totality of pores occupied by active material as a filamentary structure. Before the reaction filament thickness is r_0 and density of active material is ρ. After the reaction the products expand to occupy a cylindrical region of radius R_0 and density ρ_p. We have

$$\left(\frac{R_0}{r_0}\right)^2 = \frac{\rho}{\rho_п}. \tag{6.1}$$

Taking the density of the reaction products to be that of air at 2000–3000 K and the initial density of active material to be $\rho \sim 1$ g/cm^3 we obtain $R_0/r_0 \sim 100$.

The wave of reaction-induced combustion propagates mainly because the products expand, but the reaction is still based on the combustion of solid (adsorbed) material. Let v_0 be the velocity of the combusion wave through solid material. Then the reaction wave travels through the filament at velocity

$$v = \frac{R_0}{r_0} v_0 \sim 100 v_0. \tag{6.2}$$

For the sake of concreteness we will use a flare compound to model the active material in ball lightning. Since the combustion wave in flare compounds travels at a speed $v_0 \sim 1$ cm/s[79] then, according to equation (6.2), the speed of propagation of chemical reaction and luminescence waves should in this case be

$$v \sim 100 \text{ cm/s}.$$

The chemical reaction wave propagates along a filament of active material and creates a hot gas cylinder (which may contain solid particles as well). This cylinder[3)] luminesces because of its high temperature and cools because of thermal conduction in the gas. The length of the luminous cylinder is $l \sim v\tau$ where τ is the characteristic cooling time.

It is useful to evaluate the size of the luminous region by considering the magnitude of the ball lightning's light output—the ratio of the power of the radiant flux to the total power consumption. Clearly if the radius of the luminous region is small then the energy contained in the hot gas will quickly dissipate because of large temperature gradients. This implies that light output increases with the radius of the luminous region. Let us turn to the results of estimates of the resonance emission of sodium atoms in air heated to 2000–3000 K.[75] In this case resonance emission is confined and the light output depends on the sodium concentration c and radius of the luminous column r according to the relation

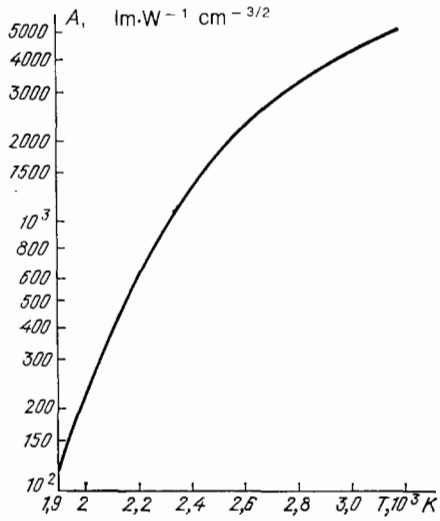

FIG. 8. The function $A(T)$ in formula (6.3) for the luminescence of a hot column containing sodium additives.

$$\eta = A(T) r^{3/2} c^{1/2}. \tag{6.3}$$

The coefficient $A(T)$ is plotted for the case when l/r of the luminous column is 50 in Fig. 8 for 2000–3000 K temperature range. It appears that the light output of ball lightning, 0.7 lm/W, corresponds to a luminous region with radius $R_0 \sim 0.01$ cm, which agrees with the initial volume occupied by active material $r_0 \sim 1\ \mu$m.[4)]

Let us evaluate other parameters of the process in given circumstances. The thermal power emitted by an individual branch of the propagating wave is $p \sim Q\rho\pi r_0^2 v \sim 0.04$ W, where $Q = 6$ kJ/g is the specific energy content, $\rho = 2$ g/cm^3 is the mass density of material (parameters of a flare compound). Since the full power of an average ball lightning is 2 kW, the number of simultaneously luminous regions is $n \sim 5 \cdot 10^4$. Further, the characteristic cooling time for regions of this size is $\tau \sim 10^{-3}$ s at $T = 2500$ K, so the length of the luminous column is $l \sim v\tau \sim 0.1$ cm and its area is $s = 2\pi R_0 l \sim 6 \cdot 10^{-3}$ cm^2, i.e., the total luminous surface is $S = sn \sim 300$ cm^2 which is an order of magnitude smaller than the surface area of a ball lightning. This indicates that the light emitted by each region freely escapes from the system without impinging on other luminous regions.

Let us now investigate another method of filling the aerogel pores with active material. Here the active material does not form a single cluster, but fills individual, unconnected pores. It is then convenient to model the active material inside the aerogel as a collection of separate spherical structures. The combustion of an individual element is accompanied by luminescence: in Fig. 9(a) we plot the radius of these structures necessary to produce a ball lightning's

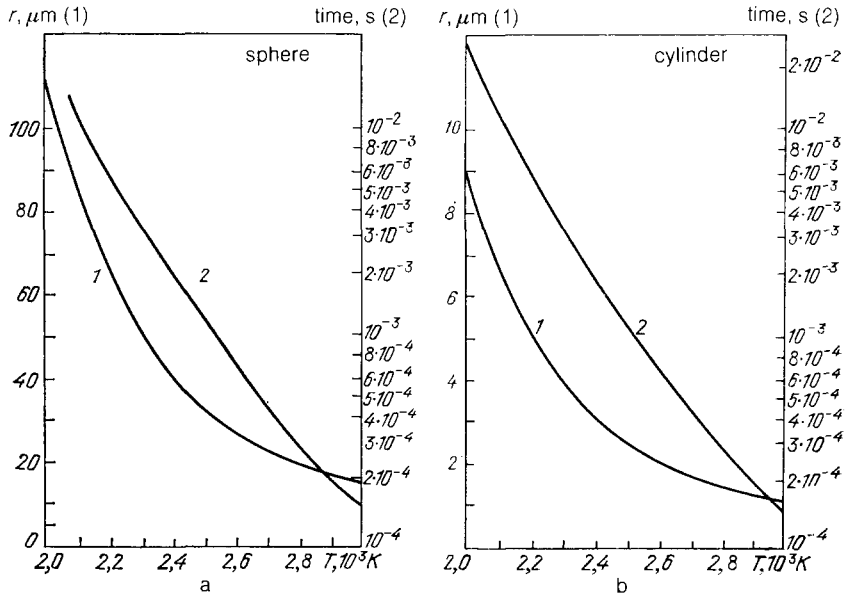

FIG. 9. Radius of the active material region and luminescence time as functions of temperature when the luminous region is spherically (a) or cylindrically (b) symmetric. The luminescence is due to resonant emission of sodium atoms whose concentration in the hot region is 1%. The parameters of the luminous region are chosen such that the light output (the ratio of radiant flux to radiated power) corresponds to the 0.7 lm/W of ball lightning.

light output when the sodium concentration is $c = 1\%$. (Note that the average concentration of sodium in the earth's crust is $c = 2.6\%$.[85]) The time τ that characterizes the period of luminescence is plotted in the same figure. Figure 9(b) illustrates analogous results for the cylindrical system. Evidently, to supply the required light output in the cylindrical system the active material should occupy pores that are an order of magnitude smaller than in the spherical system.

The physical difficulty encountered in this second method involves the propagation of the combustion wave. One possibility is to suppose that an individual element undergoes combustion when its temperature reaches some threshold value. Since the temperature front expands in all directions, the volume of the chemical reaction increases with time and the whole process becomes explosive. This is in principle different from the reaction propagation discussed earlier, where in steady state the chemical reaction propagated simultaneously along many active material filaments and the luminous volume in principle remained constant.

It should be noted that the luminosity wave propagation in certain directions may occur also when the active material is present in unconnected structures. Some complication should be incorporated in the model: for instance, water could occupy part of the pores and extinguish the temperature wave, permitting it to propagate only in certain directions. The earlier mechanism for the propagation of the luminosity wave is then recovered and both methods of filling the pores with active material result in identical luminescence.

In summation, our model of ball lightning appears thus. The ball lightning skeleton is made up of a dilute aerogel. Some micron-sized pores contain active material. The chemical reaction involving this active material heats the surrounding volume and gives rise to luminescence. At any given time there exist many luminous, microscopic regions, giving the impression of volume luminosity. This model is based on a more general phenomenological description of ball lightning;[29,75] specific aerogel information made it possible to examine some of the aspects in more detail. Since the model is free of fundamental contradictions it deserves further development.

7. CONCLUSIONS

The aerogel is an interesting physical object with unusual properties. Although it was first discovered more than fifty years ago, the aerogel still attracts less scientific interest than it deserves. This is largely due to the difficulty of its production and the resulting relatively high cost. The applications of aerogels have thus been limited, accordingly downgrading its interest as a physical object.

But let us examine the aerogel from a different viewpoint. The aerogel has a specific, cluster-like structure, consisting of small, interconnected particles; at small length scales its cluster structure is fractal. The aerogel is characterized by large specific internal surface area and large capacity—the pores occupy a volume many times greater than the solid material. At the same time, aerogels are mechanically strong and can survive high temperatures. Hence the aerogel is a normal, rather than exotic, object and should be treated as such.

Another aspect of the problem should be remarked upon. The aerogel is formed by the solid phase precipitating from solution. Its structure demonstrates that the new phase does not grow as a solid mass near a condensation center—which is the usual process—but rather as a gel with corresponding structure. Hence, gel formation is another method of forming a new phase that is characteristic for a certain class of phenomena. This process might also serve as an intermediate step in the formation of other solid phases where it is not observed because the gel is insufficiently stable. But as an intermediate step it may influence the final properties of the subsequent solid mass and therefore should be studied and understood. The information pertaining to the formation and structure of aerogels may be useful in this regard. In this fashion, aerogel formation may serve as a good model in investigating various phenomena involved in the formation

of solid phases that occur in the physics of solutions, surfaces, and biophysics.

Consequently the aerogel deserves attention not only as a real physical object with specific properties, but also as a structure which is formed in a number of physical, physical-chemical, and biophysical phenomena. More detailed study of this object may yield much that is interesting.

[1)] In this method the particles are "tinted" with metal oxides which preferentially stick to larger particles. Therefore scanning electron microscopy (SEM) favors larger particles and the mean radius measured by this method is exaggerated. This was remarked upon also in other studies (for instance, Ref. 25).

[2)] It was asserted in Ref. 45 that a large contribution to light scattering by silica aerogel is made by chlorine atoms incorporated in the aerogel. These atoms are produced by the dissociation of hydrogen chloride which is added in small quantities to the solution as a catalyst.

[3)] In fact it is shaped like a cone that is disintegrating at the base.

[4)] Recall that if the characteristic size of the particles which make up the aerogel skeleton is $r_0 = 3$ nm. Then according to formula (3.3) the characteristic pore size in an aerogel with specific gravity comparable to air is $\bar{R} \sim 100\,\mu$m for fractal dimensionality $D = 2.1$ and $\bar{R} \sim 100\,\mu$m for fractal dimensionality $D = 2.3$.

[1]S. S. Kistler, Nature **127**, 741 (1931).
[2]S. S. Kistler, J. Phys. Chem. **34**, 52 (1932); **46**, 19 (1942).
[3]S. S. Kistler and A. Cadwell, Ind. Eng. Chem. **26**, 658 (1934).
[4]S. S. Kistler, J. Chem. Phys. **39**, 79 (1935).
[5]J. Fricke, in *Aerogels*, edited by J. Fricke, Springer-Verlag, New York, 1986, p.2.
[6]S. J. Teichner, *ibid.* p. 22.
[7]G. M. Pajonk and S. J. Teichner, *ibid.*, p. 193.
[8]P. Lecomptr *et al.*, Phys. Scripta **23**, 376 (1981).
[9]G. Poelz and R. Riethmuller, Nucl. Instrum. Methods **195**, 491 (1982).
[10]G. Poelz, in *Aerogels*, edited by J. Fricke, Springer-Verlag, New York, 1986, p. 176.
[11]A. A. Vedenov, Physics of Solutions (in Russian), Nauka, M., 1984.
[12]S. J. Teichner *et al.*, Adv. Colloid. Interface Sci. **5**, 245 (1976).
[13]M. Astier *et al.*, in *Preparation of Catalysts*, edited by B. Delmon *et al.*, Elsevier, Amsterdam, 1976, p. 315.
[14]C. J. Brinker *et al.*, in *Aerogels*, edited by J. Fricke, Springer-Verlag, New York,1986, p. 2.
[15]H. Schmidt and H. Scholze, *ibid.*, p. 49.
[16]T. Woignier, J. Phalippou, and J. Zarzucky, J. Non-Cryst. Solids **63**, 117 (1984).
[17]R. K. Iler, *The Chemistry of Silica*, J. Wiley, New York, 1979.
[18]G. A. Nicolaon and S. J. Teichner, Bull. Soc. Chim. France **1968**, 1900; *ibid.*, 1906.
[19]M. Nogani and Y. Moriya J. Non-Cryst. Solids **37**, 191 (1980).
[20]P. H. Tewari, A. J. Hunt, and K. D. Lofftus in *Aerogels*, edited by J. Fricke, Springer-Verlag, New York, 1986, p. 31.
[21]C. M. Lampert and J. H. Mazur, *ibid.*, p. 154.
[22]K. C. Chen, T. Tsuchiya, and J. D. Mackenzie, J. Non-Cryst. Solids **81**, 227 (1986).
[23]P. H. Tewari *et al.*, in *Aerogels*, edited by J. Fricke, Springer-Verlag, New York, 1986, p. 142.
[24]J. B. Blum and J. W. Ryan, J. Non-Cryst. Solids **81**, 226 (1986).
[25]S. Henning and L. Svensson, Phys. Scripta, **23**, 697 (1981).
[26]S. Henning, *ibid.*, 703 (1981).
[27]S. Henning *et al.*, in *Aerogels*, edited by J. Fricke, Springer-Verlag, New York, 1986, p. 38.
[28]C. Fernandez *et al.*, Nucl. Instrum. Methods **225**, 313 (1984).
[29]B. M. Smirnov, Usp. Fiz. Nauk **149**, 177 (1986) [Sov. Phys. Usp. **29**, 481 (1986)].
[30]P. Pfeifer and D. Avnir, J. Chem. Phys. **79**, 3558 (1983).
[31]D. Avnir, D. Farin, and P. Pfeifer, *ibid.*, 3566 (1983).
[32]D. W. Schaefer *et al.*, Phys. Rev. Lett. **52**, 2371 (1984).
[33]D. W. Schaefer and K. D. Keefer, *ibid.* **53**, 1383 (1984).
[34]G. Schuck, W. Dietrich, and J. Fricke, in *Aerogels*, edited by J. Fricke, Springer-Verlag, New York, 1986, p. 148.
[35]F. J. Broecker *et al.*, ibid., p. 160.
[36]M. Cantin *et al.*, Nucl. Instrum. Methods **118**, 177 (1974).
[37]M. Bourdinaud, J. B. Cheze, and J. C. Thevenin, *ibid.* **136**, 99 (1976).
[38]A. M. Mulder and J. G. van Lierop, in *Aerogels*, edited by J. Fricke, Springer-Verlag, New York, 1986, p. 68.
[39]C. J. Brinker and G. W. Scherer J. Non-Cryst. Solids **70**, 301 (1985).
[40]M. Benot *et al.*, Nucl. Instrum. Methods **154**, 253 (1978).
[41]D. Deptuck, J. P. Harrison, and P. Zawadzki, Phys. Rev. Lett. **54**, 913 (1985).
[42]M. Gronauer, A. Kadur, and J. Fricke, in *Aerogels*, edited by J. Fricke, Springer-Verlag, New York, 1986, p. 167.
[43]O. Nilsson, A. Fransson, and O. Sandberg, in *Aerogels*, edited by J. Fricke, Springer-Verlag, New York, 1986, p. 121.
[44]R. Caps and J. Fricke, Int. J. Sol. En. **3**, 13 (1984).
[45]K. Susa *et al.*, J. Non-Cryst. Solids **79**, 165 (1986).
[46]L. D. Landau and E. M. Lifshitz, Theory of Elasticity, Pergamon Press, New York, 1986 [Russ. original, Nauka, M., 1965, p. 131].
[47]H. Burkhardt *et al.*, Nucl. Instrum. Methods **184**, 319 (1981).
[48]P. J. Carlson *et al.*, Phys. Scripta **23**, 708 (1981).
[49]H. Dislich and P. Hinz, J. Non-Cryst. Solids **48**, 11 (1982).
[50]H. Dislich, *ibid.* **73**, 599 (1985).
[51]J. Zarzycki and H. Wognier, in *Aerogels*, edited by J. Fricke, Springer-Verlag, New York, 1986, p. 42.
[52]H. Dislich, J. Non-Cryst. Solids **80**, 115 (1986).
[53]C. Arnault *et al.*, Phys. Scripta **23**, 710 (1981).
[54]T. Tanaka, Sci. Am. **244**, 110 (1981).
[55]T. A. Witten and L. M. Sander, Phys. Rev. Lett. **47**, 1400 (1981).
[56]P. Meakin, *ibid.* **51**, 1119 (1983).
[57]M. Kolb, R. Botet, and R. Jullien, *ibid.*, 1123 (1983).
[58]M. V. Smoluchowski, Z. Phys. **17**, 585 (1916).
[59]H. L. Green and W. R. Lane, Particulate Clouds: Dusts, Smokes and Mists, Van Nostrand, Princeton, N.J., 1964 [Russ. transl., Khimiya, L., 1972, p. 147].
[60]L. D. Landau and E. M. Lifshitz, *Fluid Mechanics*, Pergamon Press, New York, 1986. [Russ. original, Nauka, M., 1986].
[61]J. Weznel, J. Non-Cryst. Solids **73**, 693 (1985).
[62]A. D. Linney and B. Peters, Nucl. Instrum. Methods **100**, 545 (1973).
[63]L. Koch-Miramond and J. P. Meyer, Adv. Space. Res. **4**, 79 (1984).
[64]L. Koch-Miramond, in *Aerogels*, edited by J. Fricke, Springer-Verlag, New York, 1986, p. 188.
[65]M. Formenti *et al.*, Bull. Soc. Chim. France **1972**, 69.
[66]S. Abouarnadasse *et al.*, Appl. Catalys. **9**, 119 (1984).
[67]S. Abouarnadasse *et al.*, Can. J. Chem. Eng. **62**, 521 (1984).
[68]J. P. De Brion *et al.*, Nucl. Instrum. Methods **179**, 61 (1981).
[69]A. Goetzberger and V. Wittwer, in *Aerogels*, edited by J. Fricke, Springer-Verlag, New York, 1986, p. 84.
[70]J. Fricke, *ibid.*, p. 94.
[71]D. Büttner *et al*, *ibid.*, p. 104.
[72]W. Platzer, V. Wittwer, and M. Mielke, *ibid.*, p. 127.
[73]E. Schreiber, E. Boy, and K. Bertsch, *ibid.*, p. 133.
[74]B. M. Smirnov, Plasma Chemistry, Issue 4, (in Russian), Atomizdat, M., 1976, p. 191.
[75]B. M. Smirnov, The Question of Ball Lightning (in Russian), Nauka, M., 1987.
[76]V. Ya. Aleksandrov, I. P. Borodin, E. V. Kichenko, and I. V. Podmoshenskii, Zh. Tekh. Fiz. **52**, 818 (1982) [Sov. Phys. Tech. Phys. **27**, 527 (1982)].
[77]V. Ya. Aleksandrov, E. M. Golubev, and I. V. Podmoshenskiĭ, *ibid.*, 1987 (1982) [Sov. Phys. Tech. Phys. **27**, 1221 (1982)].
[78]B. M. Smirnov, Usp. Fiz. Nauk **116**, 731 (1975) [Sov. Phys. Usp. **18**, 636 (1975)].
[79]A. A. Shidlovskii, Basic Pyrotechnics (in Russian), Mashinostroenie, M., 1973.
[80]S. R. Forrest and T. A. Witten, J. Phys. A **12**, L109 (1979).
[81]J. D. Barry, *Ball and Bead Lightning: Extreme Forms of Atmospheric Electricity*, Plenum Press, New York, 1980. [Russ. transl., Mir., M. 1983].
[82]I. P. Stakhanov, The Physical Nature of Ball Lightning (in Russian), Energoatomizdat, M., 1985.
[83]V. P. Krainov, G. P. Lebedev, A. O. Nazaryan, and B. M. Smirnov, Zh. Tekh. Fiz. **56**, 1791 (1986) [Sov. Phys. Tech. Phys. **31**, 1066 (1986)].
[84]H. Kawai *et al.*, Nucl. Instrum. Methods **228**, 314 (1985).
[85]I. Jackson, in *Landolt-Börnstein Group V.V.2a*, Springer-Verlag, New York, 1984, p. 248.
[86]D. A. Weitz and M. Oliveria, Phys. Rev. Lett. **52**, 1433 (1984).
[87]D. A. Weitz *et al.*, *ibid.* **53**, 1967 (1984).
[88]D. A. Weitz et *al.*, *ibid.* **54**, 1416 (1985).
[89]C. Aubert and D. S. Cannell, *ibid.* **56**, 738 (1986).
[90]P. Dimon *et al.*, *ibid.* **57**, 595 (1986).

Translated by A. Zaslavsky